

A High Precision, Low Turbulence Vertical Wind Tunnel for Microrobotic Testing

Arav Bhargava, Elio Challita, Harvard Microrobotics Laboratory

Introduction

Vertical wind tunnels enable controlled studies of gliding, flapping, maneuvering, and stability in both biological insects and microrobots, where aerodynamic forces are small and flows are typically laminar. Existing tunnels are often large, expensive, and tuned for higher Reynolds numbers, making them ill-suited to micro-scale regimes ($Re < 2300$).

Objective: Create a compact, low-cost, open-source vertical wind tunnel that reliably delivers uniform, low-turbulence flow within micro-scale Reynolds numbers and can be fabricated and replicated quickly to be used by microrobotics labs around the world

Many researchers have created wind tunnels that produce laminar flow by taking a rotational flow generated by a propeller and utilizing a combination of honeycomb and wire mesh filters to convert the rotational flow to a laminar flow.

We modeled after NASA and MIT guidelines for wind tunnel with minimal turbulence $< 1\%$. Their experiments showed the efficacy in reducing turbulence using a honeycomb structure with aspect ratio 6-8, cell size 3-9mm, three screens with $> 58\%$ open area with a progression from largest opening to smallest openings, and contraction nozzle at base to increase pressure moving into the first honeycomb filter.

Methods

To design the vertical wind tunnel, Fusion 360 Computer Aided Design was used to design and fabricate a FDM 3D-printed, modular design.

Mechanical layout & flow conditioning

- Flow conditioning stack: two contraction nozzles (to minimize wall/tip effects), two straight sections, two honeycomb stages (64 mm and 40 mm tall), and four 34-mesh screens at tuned axial positions to suppress large-scale turbulence and equalize the velocity profile. This is shown in Figure 1a.

Drive & control

- 335 KV brushless motor with 8x6 three-blade propeller, controlled via ESC (Figure 1c)
- Arduino-based PID loop closes the velocity feedback using an **F53000 air-velocity sensor**. This is shown in Figures 1b and 1d.
- A mount for a traditional hot-wire probe is included for future calibration and turbulence measurements.

Visualization & Particle Image Velocimetry workflow

- Particle Image Velocimetry (PIV) is performed on the laser-illuminated, glycerol-seeded images to quantify the velocity field and assess spatial uniformity and turbulence qualitatively (with parameters tuned to minimize spurious vectors).
- A 10 mW laser forms a thin planar sheet for flow visualization.
- Glycerol particles are seeded and convected around a test cylinder to reveal streamlines and potential wake structures.

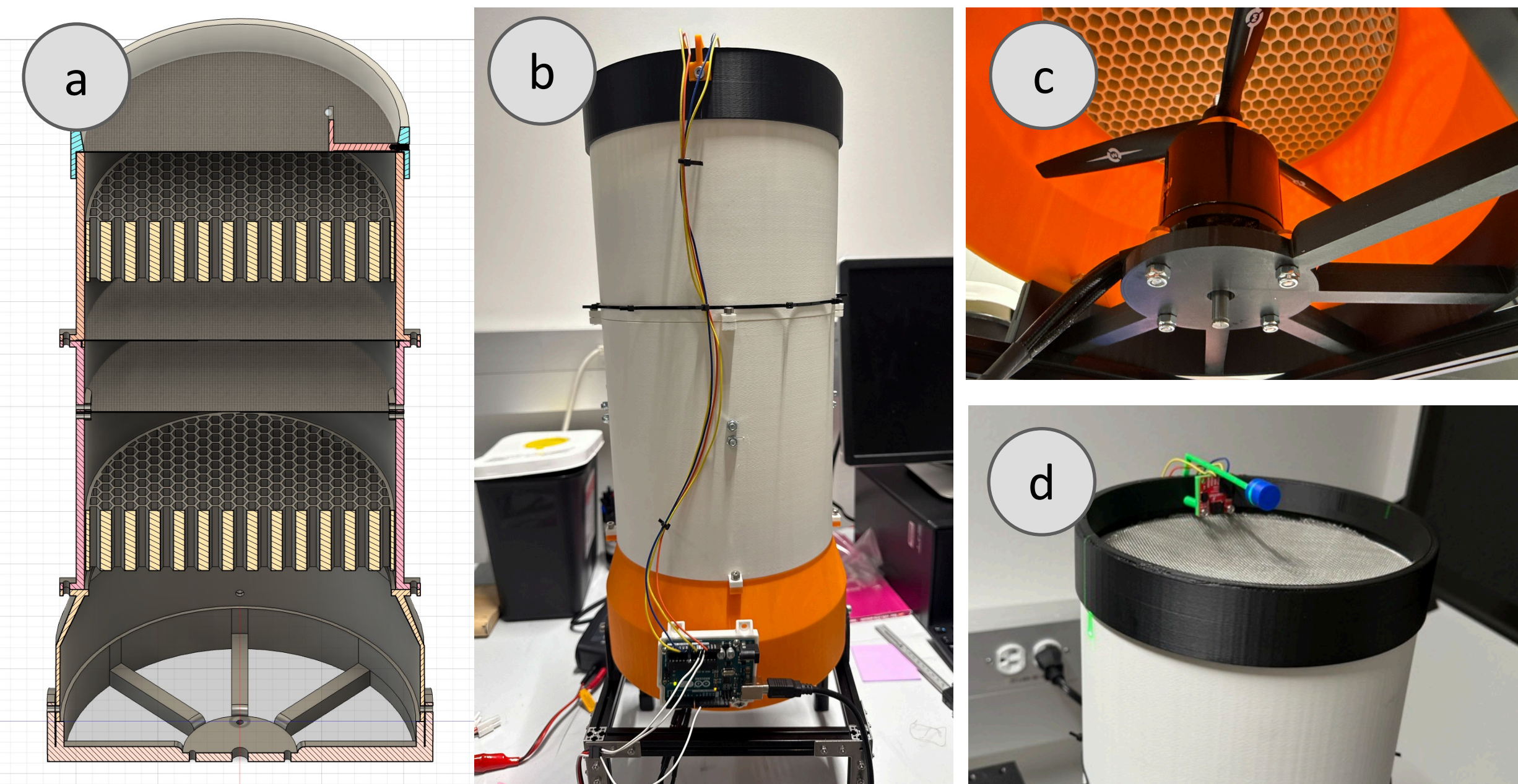


Figure 1. (a) Interior view of the vertical wind tunnel highlighting the modular, 3D-printed assembly. (b) Exterior view of the complete system, including the Arduino Uno control electronics. (c) Detail of the three-blade propeller and the first honeycomb flow straightener. (d) PIV test configuration showing the cylinder model and the F53000 air-velocity sensor.

Acknowledgements

This work was supported by a PRISE award from the Harvard College Office of Undergraduate Research and Fellowships.

Testing and Results



Figure 2. PIV testing setup with high speed camera positioned to view smoke-seeded airflow around the 10mm cylinder.

Setpoint verification at very low speed ($V = 0.28$ m/s)

Using standard air at $\sim 25^\circ\text{C}$ and 1 atm ($\rho \approx 1.18$ kg/m³, $\mu \approx 1.85 \times 10^{-5}$ Pa·s), the external Reynolds number based on cylinder/wire diameter D is:

$$Re = (\rho \cdot V \cdot D) / \mu$$

Example values at $V = 0.28$ m/s:

- $D = 5$ mm $\rightarrow Re \approx 93$
- $D = 10$ mm $\rightarrow Re \approx 186$

As shown in Figure 5, with thin cylinders of 5 and 10 mm, the flow is squarely in the steady separated laminar regime ($Re \approx 50-100$), showing a strong correlation between these calculations and our qualitative observations.

Key visual features of PIV showed at 0.28 m/s (low-Re cylinder flow)

- Uniform upstream flow:** Long, straight vectors approaching the cylinder, showing an undisturbed stream.
- Smooth diversion:** Vectors gently curve around the cylinder's surface with no abrupt separation.
- Steady recirculation bubbles:** Two small, mirror-symmetric "pockets" of very short (or upstream-pointing) vectors immediately downstream.
- No vortex shedding:** The wake remains steady and symmetric rather than oscillating side to side.
- Reattachment:** After the recirculation zones, the flow rejoins into a nearly uniform pattern again.

These characteristics indicate a classic laminar separated wake typical of Reynolds numbers around 50–100.



Figure 4. Smoke seeded airflow around 5mm cylinder at 0.35 m/s airflow. Qualitatively shows laminar flow.

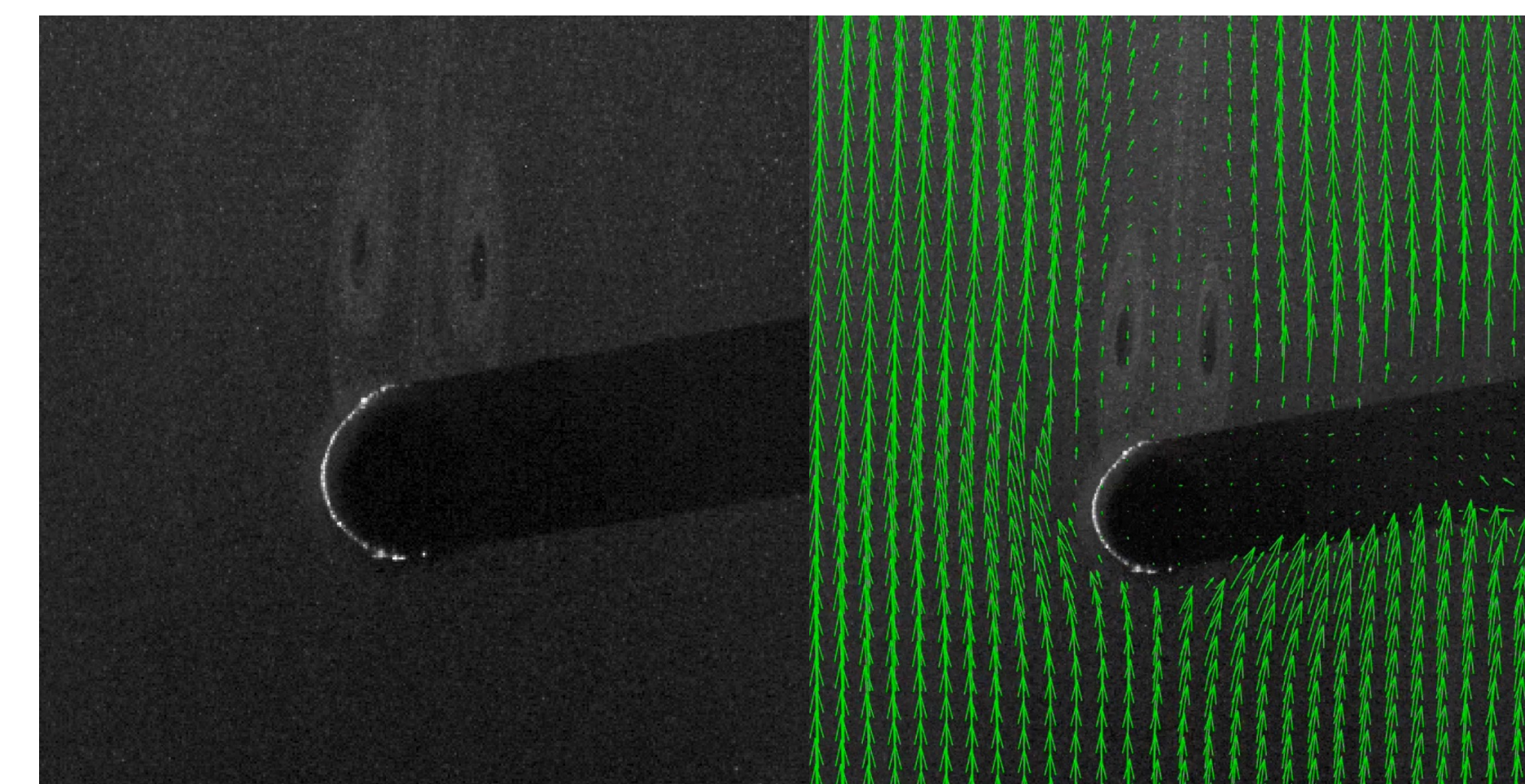


Figure 5. Side by side PIV and vector analysis of a 0.28 m/s flow. Tiny inward circulation can be seen directly above the cylinder.

Stability and repeatability

- The closed-loop controller held commanded speeds with ± 0.02 m/s resolution using computer based air velocity control.
- Using a potentiometer, the air velocity was able to be controlled in real time.

Conclusion

Vector fields in Figure 5 versus Figure 3 indicate $Re \approx 50-100$ showing a **steady laminar flow** with a **laminar Kármán wake**. Our calculations agree, confirming that a **sub-\$150, sub-600 mm system** can deliver a research-grade, low-Re environment for insect-scale and microrobotic aerodynamics.

Additionally after testing, our vertical wind tunnel has demonstrated the following capabilities:

- Precision control:** Closed-loop velocity regulation with ± 0.02 m/s setpoint resolution across **0.2–2.5 m/s**.
- Ease of Replication:** **Sub-600 mm total height, ~\$150 bill of materials**, fully open-source, buildable in **< 2 days**.

Implications for the field of microrobotics:

- Aerodynamic characterization:** Lift/drag/moment measurements for small foils and wings under uniform, low-turbulence inflow.
- System identification:** Repeatable conditions for parameter estimation and controller tuning.

Together, the PIV signatures and closed-loop control show this **compact, low-cost tunnel** is a functional platform for microrobotic performance and control experiments.

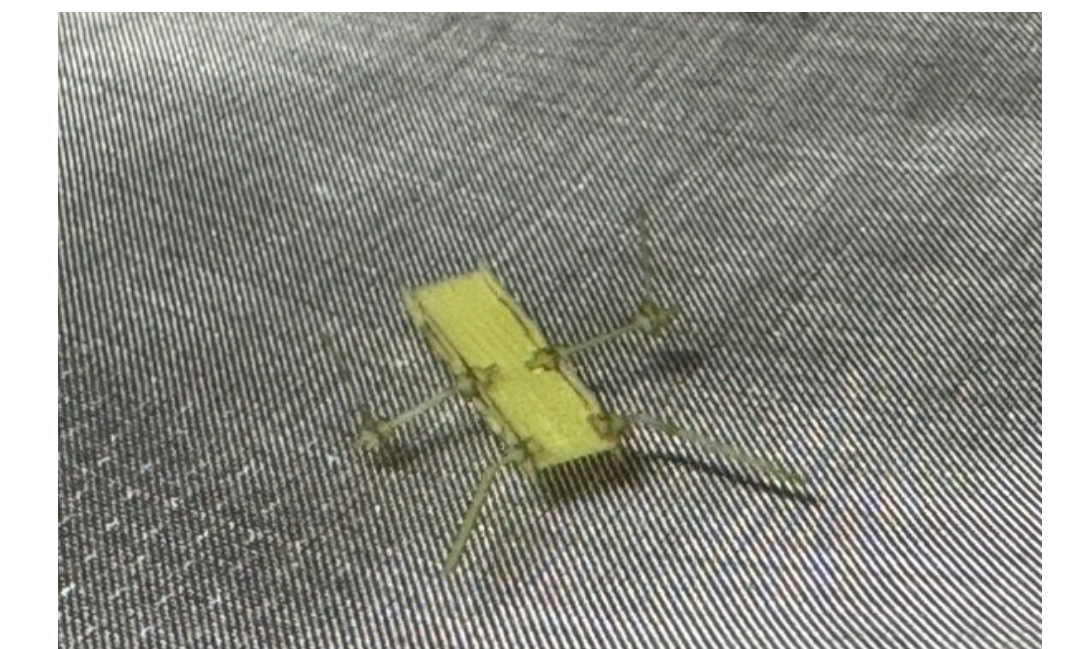


Figure 6. Harvard Microrobotics Lab robotic insect hovering above the vertical wind tunnel.

Next Steps

- Controller refinement:**
 - Characterize step response, disturbance rejection, and drift; consider feed-forward terms and sensor fusion (e.g., adding a hot-wire probe for higher bandwidth).
 - Use of camera to lower and raise air velocity when robot exists certain predetermined area
- Improving laser setup for PIV analysis:**
 - As shown in Figures 4 and 5, the laser is blocked by the cylinder, creating a shadow and gap in our data collection and PIV analysis.
 - Through the use of clear tubes with liquid carrying a similar refraction index, we can eliminate this shadow.
- Flow-conditioning optimization:**
 - Systematically vary screen/honeycomb spacing and nozzle geometry; validate turbulence vs. cost/height trade-offs.
- Application studies:**
 - Execute experiments such as stabilization studies for microrobotic flyers to demonstrate experimental breadth.

References

- NASA Technical Report [PDF] "19710004069."
<https://ntrs.nasa.gov/api/citations/19710004069/downloads/19710004069.pdf>
- Mehta, R. D., & Bradshaw, P. (1979). Design rules for small low-speed wind tunnels. *The Aeronautical Journal*.
PDF: https://ara.bme.hu/neptun/BMEGEATNG01/2022-2023-II/labor/H04_irodalom/05_LowSpeedTunnels.pdf
- Groth, J., & Johansson, A. V. (1988). Turbulence reduction by screens. *Journal of Fluid Mechanics*, 197, 139–155.
PDF: <https://www.gogab.se/wp-content/uploads/2010/04/S0022112088003209a.pdf>

Learn More

Email: abhargava@college.harvard.edu